

Dalitz-plot analysis of $B^\pm \rightarrow K^\pm K^+ K^-$ decays

L. Leśniak* and P. Żenczykowski

Division of Theoretical Physics

The Henryk Niewodniczański Institute of Nuclear Physics,

Polish Academy of Sciences

PL 31-342 Kraków, Poland

May 29, 2024

Abstract

We study $B^\pm \rightarrow K^\pm K^+ K^-$ decays using the QCD factorization model with final state interactions between K^+ and K^- mesons taken into account. The parameters of the model are fitted to the data of the *BABAR* and LHCb collaborations. We describe the $K\bar{K}$ effective mass distributions and examine the CP -violating asymmetry effects in the full range of the Dalitz plot.

PACS numbers: 13.25.Hw, 13.75.Lb

*email: leonard.lesniak@ifj.edu.pl

1 Introduction

Theoretical understanding of CP violation effects in B weak decays requires proper description of both weak and strong phases of the decay amplitudes. The latter are in principle determined by the short- and long-distance QCD interactions. While the two-body B decays provide the simplest setting for the study of the interplay of weak and strong interactions, their three-body decays call for the analysis of more complicated strong interaction effects that may lead to significant variability of CP -asymmetry in the Dalitz plots. With the relevant effects being induced by various long-distance contributions (such as final state interactions (FSI)), their description is difficult and requires the use of QCD-inspired models.

Of particular interest are here the three-body B decays into light mesons such as $B \rightarrow \pi\pi\pi$, $\pi\pi K$, πKK , KKK . The long-distance strong interactions include both the resonant and nonresonant contributions (see [1],[2]) that may be mutually interfering and could be described as proceeding through a quasi-two-body stage $B \rightarrow M_1 M_2$ with meson M_2 ultimately decaying into two final-state mesons m and m' . The description of the relevant induced invariant-mass-dependent effects calls for the careful consideration of both the resonances and their interferences in the low-mass regions of the Dalitz plot such as $\rho(770)$, $\omega(782)$, $f_0(980)$, $\phi(1020)$, $f_2(1270)$, $\omega(1420)$, $\rho(1450)$, $f'_2(1525)$, *etc.* ([3]-[6]) as well as various hadronic loop or penguin contributions. The latter may involve the $\pi\pi \rightarrow KK$ rescattering as discussed in [7]-[10] and the effects of charm $D\bar{D}$ threshold opening up at higher invariant masses [11],[12].

In our work in the past (see [7], [13], [14]) we concentrated on an analysis of the $B^\pm \rightarrow K^\pm K^+ K^-$ decays [15]-[17], using the quasi-two-body QCD factorization model [18] with some FSI added. The $K^+ K^-$ rescattering effects were restricted to fairly low values of the $K\bar{K}$ invariant mass. The availability of the experimental data in the region of the large effective mass values of the interacting $K^+ K^-$ pair, and a large variability of CP asymmetry in the Dalitz plot as observed by *BABAR* and LHCb [16],[19],[20], are important as they put stringent constraints on the theoretical models. It is therefore challenging to extend our previous work and describe the $B^\pm \rightarrow K^\pm K^+ K^-$ decays in the full range of the Dalitz plot. Such an extension of our model constitutes the subject of the present paper.

We present our extended model in Sec. 2 where the relevant amplitudes are defined. The Dalitz plot distributions are discussed in Sec. 3. Various parameters and the fitting procedure are described in Sec. 4. Our results are given in Sec. 5. Summary and final comments can be found in Sec. 6.

2 Amplitudes of the $B^\pm \rightarrow K^\pm K^+ K^-$ decays

In this chapter we widen our studies of the $B^\pm \rightarrow K^\pm K^+ K^-$ decays presented in Refs. [7], [13] and [14]. We employ the quasi-two-body QCD factorisation model [18] of the decay amplitudes extending it to large effective $K\bar{K}$ masses. In order to

describe the full range of these masses, up to about 4.78 GeV, the relevant decay amplitudes have to be modified. In this section we give general theoretical expressions for the decay amplitudes. Our modifications will be introduced in the subsequent sections.

The amplitude $A^-(s_{12}, s_{23})$ for the $B^- \rightarrow K^-(p_1)K^+(p_2)K^-(p_3)$ decay is a function of two $K\bar{K}$ invariant masses squared: $s_{12} = (p_1 + p_2)^2$ and $s_{23} = (p_2 + p_3)^2$, where p_1 , p_2 and p_3 are the kaon four-momenta. This decay amplitude has to be symmetrized as in the final state two kaons of negative charge are emitted. The symmetrized amplitude A_{sym}^- is

$$A_{sym}^- = \frac{1}{\sqrt{2}}[A^-(s_{12}, s_{23}) + A^-(s_{23}, s_{12})]. \quad (1)$$

The amplitude $A^-(s_{12}, s_{23})$ is a sum of six components A_i^- :

$$A^-(s_{12}, s_{23}) = \sum_{i=1}^6 A_i^-, \quad (2)$$

where

$$A_1^- = \frac{G_F}{\sqrt{2}} \nu \frac{2B_0}{m_b - m_s} (M_B^2 - m_K^2) F_0^{B^- K^-}(s_{23}) \Gamma_2^{s*}(s_{23}), \quad (3)$$

$$A_2^- = -\frac{G_F}{\sqrt{2}} y \sqrt{\frac{1}{2}} f_K (M_B^2 - s_{23}) F_0^{B^- \rightarrow (K^+ K^-)_S}(m_K^2) [\chi \Gamma_2^{n*}(s_{23}) + G_1(s_{23})], \quad (4)$$

$$A_3^- = \frac{G_F}{\sqrt{2}} (s_{12} - s_{13}) F_1^{B^- K^-}(s_{23}) \left[w_u F_u^{K^+ K^-}(s_{23}) + w_s F_s^{K^+ K^-}(s_{23}) \right], \quad (5)$$

$$A_4^- = -\frac{G_F}{\sqrt{2}} y \frac{f_K}{f_\rho} (s_{12} - s_{13}) A_0^{B^- \rho^0}(m_K^2) F_u^{K^+ K^-}(s_{23}), \quad (6)$$

$$A_5^- = -\frac{G_F}{\sqrt{2}} y f_K D(s_{12}, s_{23}) \langle f_2 | u\bar{u} \rangle G_{f_2 K^+ K^-}(s_{23}) F^{B^- f_2}(m_K^2), \quad (7)$$

and

$$A_6^- = -\frac{G_F}{\sqrt{2}} y f_K D(s_{12}, s_{23}) \langle f_2' | u\bar{u} \rangle G_{f_2' K^+ K^-}(s_{23}) F^{B^- f_2'}(m_K^2). \quad (8)$$

The amplitudes A_1^- and A_2^- depend on the $K^+ K^-$ interactions in the S -wave, the A_3^- and A_4^- terms constitute the P -wave components, while the amplitudes A_5^- and A_6^- involve the D -wave resonances $f_2(1270)$ and $f_2'(1525)$. All the amplitudes are proportional to the Fermi coupling constant G_F . They also depend on QCD factorization coefficients a_j^c and a_j^u ($j=1, \dots, 10$), and on the products $\Lambda_u = V_{ub} V_{us}^*$,

$\Lambda_c = V_{cb}V_{cs}^*$, where V_{kl} are the CKM quark-mixing matrix elements. These coefficients as well as Λ_u and Λ_c enter in the factors ν , y , w_u and w_s present in Eqs. (3)-(8). They are defined as follows:

$$\nu = \Lambda_u(-a_{6\nu}^u + \frac{1}{2}a_{8\nu}^u) + \Lambda_c(-a_{6\nu}^c + \frac{1}{2}a_{8\nu}^c), \quad (9)$$

$$y = \Lambda_u \left[a_{1y} + a_{4y}^u + a_{10y}^u - (a_{6y}^u + a_{8y}^u)r_\chi^K \right] + \Lambda_c \left[a_{4y}^c + a_{10y}^c - (a_{6y}^c + a_{8y}^c)r_\chi^K \right], \quad (10)$$

where

$$r_\chi^K = \frac{2m_K^2}{(m_b + m_u)(m_u + m_s)}, \quad (11)$$

$$w_u = \Lambda_u(a_{2w} + a_{3w} + a_{5w} + a_{7w} + a_{9w}) + \Lambda_c(a_{3w} + a_{5w} + a_{7w} + a_{9w}), \quad (12)$$

and

$$w_s = \Lambda_u \left[a_{3w} + a_{4w}^u + a_{5w} - \frac{1}{2}(a_{7w} + a_{9w} + a_{10w}^u) \right] + \Lambda_c \left[a_{3w} + a_{4w}^c + a_{5w} - \frac{1}{2}(a_{7w} + a_{9w} + a_{10w}^c) \right]. \quad (13)$$

The masses of the B^\pm and the K^\pm mesons and those of the b -quark, u -quark, d -quark and the strange quark are denoted as M_B , m_K , m_b , m_u , m_d , and m_s , respectively. The values of the coefficients a_j , a_j^c and a_j^u , calculated at next-to-leading order, are given in Table 1 of Ref. [13].

The constant B_0 in the amplitude A_1^- (Eq. 3) is defined as $B_0 = m_\pi^2/(m_u + m_d)$, where m_π is the mass of the charged pion. The function $F_0^{B^-K^-}(s_{23})$ is the $B^- \rightarrow K^-$ scalar transition form factor. We follow Ref. [22] and parameterize it as $F_0^{B^-K^-}(s) = r_0/(1 - s/s_0)$, where $r_0 = 0.33$ and $s_0 = 37.46 \text{ GeV}^2$.

The function $\Gamma_2^s(s_{23})$ is the kaon strange scalar form factor. In its calculation the knowledge of the strong $K\bar{K}$ interactions as well as the interactions in the meson channels coupled to K^+K^- (like the $\pi\pi$ and four pion systems) is needed. A unitary model of the S -wave $\pi\pi$, $K\bar{K}$ and the 4π amplitudes has been developed in Refs. [23] and [24]. Recently, it has been updated using some new experimental data (see Appendix A in Ref. [25]). The coupling of the four pion channel to the $K\bar{K}$ channel becomes important when the corresponding K^+K^- effective mass exceeds a value of about 1300 MeV. It is known that two scalar resonances $f_0(1370)$ and $f_0(1500)$ have large decay branching fractions into four pions [26]. The four pions can form clusters of two-pion systems like $\rho\rho$ or $\sigma\sigma$ and their interactions can lead to an enhancement of the $K\bar{K}$ mass distribution near 1.5 GeV.

Applying the above three-channel model and the Muskhelishvili-Omnes dispersion relations Bachir Moussallam [27] has calculated the kaon strange scalar form

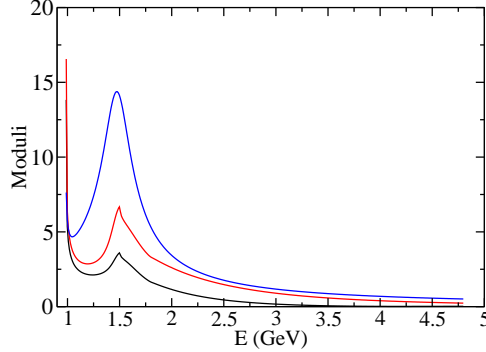


Figure 1: Moduli of the kaon scalar strange form factor $\Gamma_2^s(s)$ (black line), the kaon scalar non-strange form factor $\Gamma_2^n(s)$ (red line), and the transition function $G_1(s)$ divided by the constant χ (blue line) plotted as functions of $E = \sqrt{s}$.

factor $\Gamma_2^s(s_{23})$ and the non-strange scalar form factor $\Gamma_2^n(s_{23})$ which appears in the amplitude A_2^- (Eq. (4)). At this stage some additional assumptions about an asymptotic behaviour of the phase shifts for the centre of mass energy above 1.8 GeV have been necessary since in that energy range no experimental data on the meson-meson interactions are available. Labelling by $i = 1$ the pion-pion channel, by $i = 2$ the $K\bar{K}$ channel and by $i = 3$ the effective $2\pi 2\pi$ channel the asymptotic limits of the phase shifts δ_{ii} have been taken as 2π , π and 0, respectively for i equal to 1, 2 and 3.¹

The amplitude A_2^- involves the charged kaon decay constant f_K and the transition form factor $F_0^{B^- \rightarrow (K^+K^-)s}(m_K^2)$ from the B^- meson to the K^+K^- pair in the S -wave. As in Ref. [28] we take its value as 0.13. One also has the kaon non-strange scalar form factor $\Gamma_2^n(s_{23})$ multiplied by the constant χ related to the decay strength of the intermediate S -wave state into K^+K^- pair. In comparison with a set of the S -wave amplitudes used in Ref. [14] a new component of the A_2^- amplitude proportional to the function $G_1(s_{23})$ appears in Eq. (4). In this component a transition from the $u\bar{u}$ pair of quarks into the K^+K^- spin zero isospin one state is included. Its strength is given by a complex coupling constant r_2 which will be fitted to data.

The transition function $G_1(s_{23})$ has been defined in Ref. [25] and used in the description of the $D^0 \rightarrow K_S^0 K^+ K^-$ decays where the K^+K^- pair also appears in the final state. A coupling of the S -wave isospin one $\pi\eta$ state to the K^+K^- state enters in a derivation of the transition function G_1 . The $\pi\eta$ and the K^+K^- states have been introduced in a unitary way. The G_1 function has two poles related to the scalar-isovector resonances $a_0(980)$ and $a_0(1450)$. In the present application the

¹In Appendix A of Ref. [25] these asymptotic limits have been taken as 3π , π and $-\pi$ what changed a behaviour of the kaon form factors.

ratio of the $\pi\eta$ coupling to the K^+K^- coupling equal to 0.88 is taken from [25].

In Fig. 1 the moduli of the form factors $\Gamma_2^s(s)$ and $\Gamma_2^n(s)$, and the transition function $G_1(s)$ divided by the constant χ are shown. As seen in Eq. (4) this division is necessary since both χ and $G_1(s)$ have dimension GeV^{-1} while the kaon form factors are dimensionless.

The P -wave amplitude A_3^- depends on the charged kaon decay constant f_K and on the B^- to K^- vector transition form factor $F_1^{B^-K^-}(s_{23})$. Its form is taken from [22] as

$$F_1^{BK}(s) = \frac{r_1}{1 - \frac{s}{m_1^2}} + \frac{r_2}{(1 - \frac{s}{m_1^2})^2}, \quad (14)$$

where $r_1 = 0.162$, $r_2 = 0.173$ and $m_1 = 5.41$ GeV.

In Eq. (5) there are two terms with the functions $F_u^{K^+K^-}(s_{23})$ and $F_s^{K^+K^-}(s_{23})$. The first term describes the transitions from the $u\bar{u}$ pair of quarks into a set of ρ and ω resonances, while the second - the $s\bar{s}$ transitions into the $\phi(1020)$ and the $\phi(1680)$ resonances. Among the ρ mesons we include three states: $\rho(770)$, $\rho(1450)$ and $\rho(1700)$, labelled by $i = 1, 2, 3$, respectively. In addition we add three isospin zero resonances: $\omega(782)$, $\omega(1420)$ and $\omega(1650)$ indicated by $i = 4, 5, 6$. Thus the $F_u^{K^+K^-}(s_{23})$ function is parametrized as follows:

$$F_u^{K^+K^-}(s_{23}) = \sum_{i=1}^6 b_i BW_i(s_{23}). \quad (15)$$

where b_i are complex constants to be fitted to experimental data. The Breit-Wigner functions read:

$$BW_i(s_{23}) = \frac{m_i^2}{m_i^2 - s_{23} - i\sqrt{s_{23}}\Gamma_i(s_{23})}. \quad (16)$$

Here m_i are masses of the six vector mesons mentioned above and $\Gamma_i(s_{23})$ are their energy dependent widths

$$\Gamma_i(s_{23}) = \frac{m_i^2}{s_{23}} \left(\frac{p}{p_i}\right)^3 \Gamma_i \quad (17)$$

with Γ_i being the total widths of resonances and the momenta p and p_i defined as

$$p = \frac{1}{2}\sqrt{s_{23} - 4m_K^2}, \quad p_i = \frac{1}{2}\sqrt{m_i^2 - 4m_K^2}. \quad (18)$$

Using the isospin symmetry for the ρ and ω resonances we put $b_4 = b_1$, $b_5 = b_2$ and $b_6 = b_3$ thus reducing the number of model parameters.

The $F_s^{K^+K^-}(s_{23})$ function is defined in a similar way as $F_u^{K^+K^-}(s_{23})$ in Eq. (15):

$$F_s^{K^+K^-}(s_{23}) = b_\phi BW_\phi(s_{23}) + b_{\phi'} BW_{\phi'}(s_{23}). \quad (19)$$

Here the indices ϕ and ϕ' label the resonances $\phi(1020)$ and $\phi(1680)$, respectively. We treat b_ϕ as a real fitted parameter and take $b_{\phi'} = 0.018$ using Table 2 of Ref. [29].

The term corresponding to a transition from the $d\bar{d}$ quarks into the final K^+K^- pair and present in Eq. (3) of Refs. [13] and [14] has been omitted since the two charged kaons have no $d\bar{d}$ constituents and therefore the $d\bar{d} \rightarrow K^+K^-$ transition should be suppressed with respect to the $u\bar{u} \rightarrow K^+K^-$ transition.

The amplitude A_4^- represents the B^- transitions into the K^+K^- pairs in the P -wave. Therefore it is proportional to the vector transition form factor $A_0^{B^-\rho^0}(m_K^2)$ divided by the ρ^0 decay constant f_ρ which in our approximation effectively represents contributions of all the P -wave resonances created from the $u\bar{u}$ pairs. From Ref. [18] we take $A_0^{B^-\rho^0}(m_K^2) = 0.37$.

The amplitudes A_5^- and A_6^- depend on the function $D(s_{12}, s_{23})$ which is expressed as

$$D(s_{12}, s_{23}) = \frac{1}{3}(|\vec{p}_1| |\vec{p}_2|)^2 - (\vec{p}_1 \cdot \vec{p}_2)^2, \quad (20)$$

where \vec{p}_1 and \vec{p}_2 are the momenta of the kaons $K^-(p_1)$ and the $K^+(p_2)$ in the rest frame of $K^+(p_2)$ and $K^-(p_3)$. If one denotes $m_{23} = \sqrt{s_{23}}$ then

$$\begin{aligned} \vec{p}_1 \cdot \vec{p}_2 &= \frac{1}{4}(s_{13} - s_{12}), \\ |\vec{p}_1| &= \frac{1}{2m_{23}} \sqrt{[M_B^2 - (m_{23} + m_K)^2] [M_B^2 - (m_{23} - m_K)^2]}, \\ |\vec{p}_2| &= \frac{1}{2} \sqrt{m_{23}^2 - 4m_K^2}. \end{aligned} \quad (21)$$

Using the mixing angle $\alpha_T = (81 \pm 1)^\circ$ relevant for the quark composition of $f_2(1270)$ and $f_2'(1525)$ (see Ref. [26]) one gets

$$\langle f_2 | u\bar{u} \rangle = \frac{1}{\sqrt{2}} \sin \alpha_T \approx 0.698 \quad (22)$$

and

$$\langle f_2' | u\bar{u} \rangle = \frac{1}{\sqrt{2}} \cos \alpha_T \approx 0.111. \quad (23)$$

These factors are included in Eqs. (7) and (8), respectively.

The amplitude A_5^- is proportional to the Breit-Wigner function $G_{f_2K^+K^-}(s_{23})$ describing a coupling of the $f_2(1270)$ resonance to the final K^+K^- pair:

$$G_{f_2K^+K^-}(s_{23}) = \frac{g_{f_2K^+K^-}}{m_{f_2}^2 - s_{23} - im_{f_2}\Gamma_{f_2}}. \quad (24)$$

The coupling constant $g_{f_2K^+K^-}$ is evaluated from the expression

$$g_{f_2K^+K^-} = m_{f_2} \sqrt{\frac{60\pi\Gamma_{f_2K^+K^-}}{q_{f_2}^5}}, \quad (25)$$

where q_{f_2} is the kaon momentum in the f_2 center-of-mass frame and $\Gamma_{f_2K^+K^-} = \frac{1}{2} \cdot 4.6\% \cdot \Gamma_{f_2}$, with m_{f_2} and Γ_{f_2} being the $f_2(1270)$ mass and its total width taken

from Ref. [26]. The last factor in Eq. (7) is the effective form factor $F^{Bf_2}(m_K^2)$ for the transition of the B^- meson into $f_2(1270)$. It will be treated as a free complex parameter called further F_5 .²

The Breit-Wigner function $G_{f_2'K^+K^-}(s_{23})$ in the A_6^- amplitude from Eq. (8) is defined in a similar way as the corresponding $G_{f_2K^+K^-}(s_{23})$ function in Eqs. (24) and (25). The width for the $f_2'(1525)$ decay into K^+K^- is equal to $\Gamma_{f_2'K^+K^-} = \frac{1}{2} \cdot 88.7\% \cdot \Gamma_{f_2'}$. The effective form factor $F^{B^-f_2'}(m_K^2)$, hereafter named F_6 , will be a complex parameter to be determined from a fit to data.

The $B^+ \rightarrow K^+K^-K^+$ decay amplitude can be obtained from the A_{sym}^- amplitude written in Eq. (1) by substitutions $\Lambda_u \rightarrow \Lambda_u^*$ and $\Lambda_c \rightarrow \Lambda_c^*$ in the definitions of the coefficients v, y, w_u and w_s appearing in Eqs. (3 - 8). Moreover, one has to change B^- into B^+ and K^- into K^+ in the corresponding equations.

3 Dalitz plot distributions

The double differential branching fraction distributions which can also be called the Dalitz plot distributions for the $B^\pm \rightarrow K^\pm(p_1)K^+(p_2)K^-(p_3)$ decays are expressed by the decay amplitudes $A_{sym}^\pm(s_{12}, s_{23})$ as:

$$\frac{dBr^\pm}{ds_{12} ds_{23}} = \frac{1}{32(2\pi)^3 M_B^3 \Gamma_B} |A_{sym}^\pm(s_{12}, s_{23})|^2, \quad (26)$$

where Γ_B is the total width of the charged B meson.

As the Dalitz plot distribution is symmetric under the exchange of s_{12} and s_{23} , one can limit the integration range on s_{12} to the values larger than s_{23} . Taking this into account we introduce new names of the relevant variables, ie. $m_{K^+K^-low} = m_{23} = \sqrt{s_{23}}$ and $m_{K^+K^-high} = m_{12} = \sqrt{s_{12}}$. An additional factor of 2 is inserted in the differential effective m_{23} mass distribution:

$$\frac{dBr^\pm}{dm_{23}} = 4 m_{23} \int_{D_{12}}^{s_{12}max} ds_{12} \frac{dBr^\pm}{ds_{12} ds_{23}}. \quad (27)$$

Here D_{12} is equal to s_{12min} for $2m_K < m_{23} < d$ or $D_{12} = s_{23}$ for $d < m_{23} < M_B - m_K$, where $d = \sqrt{m_K(M_B + m_K)} \approx 1.6882$ GeV. The limits on the values of s_{12} at the border of the Dalitz plot contour for fixed values of m_{23} can be calculated in the center-of-mass frame of the $K^\pm(p_2)K^\mp(p_3)$ mesons:

$$\begin{aligned} s_{12min} &= (E_1 + E_2)^2 - (|\vec{p}_1| + |\vec{p}_2|)^2, \\ s_{12max} &= (E_1 + E_2)^2 - (|\vec{p}_1| - |\vec{p}_2|)^2, \end{aligned} \quad (28)$$

²The effective form factor for the $B \rightarrow f_2$ transition is composed of three terms which are not well known (see Eq. (10a) in Ref. [30]). Here we have to correct the values of $F^{Bf_2}(m_K^2)$ given in Table 1 of Ref. [14] for the two fits to data as they involve numerical errors. They should be rescaled down: the value 11.9 ± 1.3 should be replaced by 1.08 ± 0.12 , while the value 12.3 ± 3.5 by 1.11 ± 0.32 .

where

$$E_1 = \frac{M_B^2 - m_{23}^2 - m_K^2}{2m_{23}}, \quad |\vec{p}_1| = \sqrt{E_1^2 - m_K^2}, \quad (29)$$

$$E_2 = \frac{m_{23}}{2}, \quad |\vec{p}_2| = \sqrt{E_2^2 - m_K^2}.$$

The lower limit of m_{23} is equal to the K^+K^- threshold value $2m_K \approx 0.98735$ GeV and the upper limit is $g = \sqrt{(M_B^2 - m_K^2)/2} \approx 3.7166$ GeV.

The second branching fraction projection or the differential effective m_{12} mass distribution is given by the following expression:

$$\frac{dBr^\pm}{dm_{12}} = 4m_{12} \int_{s_{23\min}}^{G_{23}} ds_{23} \frac{dBr^\pm}{ds_{12} ds_{23}}. \quad (30)$$

In this equation m_{12} varies between the values d and $M_B - m_K$ and G_{23} is equal to m_{12}^2 for $d < m_{12} < g$ or it is equal to $s_{23\max}$ for $g < m_{12} < M_B - m_K$. The limits of the s_{23} values at fixed m_{12} can be calculated in the center-of-mass frame of the $K^\mp(p_1)K^\pm(p_2)$ mesons:

$$s_{23\min} = (E_2' + E_3)^2 - (|\vec{p}_2'| + |\vec{p}_3|)^2, \quad (31)$$

$$s_{23\max} = (E_2' + E_3)^2 - (|\vec{p}_2'| - |\vec{p}_3|)^2,$$

where

$$E_2' = \frac{m_{12}}{2}, \quad |\vec{p}_2'| = \sqrt{E_2'^2 - m_K^2}, \quad (32)$$

$$E_3 = \frac{M_B^2 - m_{12}^2 - m_K^2}{2m_{12}}, \quad |\vec{p}_3| = \sqrt{E_3^2 - m_K^2}.$$

There is also a possibility to make the third Dalitz plot projection as the differential effective m_{13} mass distribution. In the case of the $B^- \rightarrow K^-K^+K^-$ decay this is the $m_{K^-K^-}$ distribution and in the case of the $B^+ \rightarrow K^+K^+K^-$ reaction we have the $m_{K^+K^+}$ distribution. The integration formula for these distributions reads:

$$\frac{dBr^\pm}{dm_{13}} = 4m_{13} \int_x^y ds_{23} \frac{dBr^\pm(s_{12} = 2y - s_{23}, s_{23})}{ds_{12} ds_{23}}, \quad (33)$$

where $y = (M_B^2 + 3m_K^2 - s_{13})/2$, $s_{13} = m_{13}^2$ and $x = y - \sqrt{y^2 - m_K^2(M_B^2 - m_K^2)^2/s_{13}}$. Here the equality $s_{12} + s_{13} + s_{23} = M_B^2 + 3m_K^2$ has been applied.

In Ref. [19] the LHCb Collaboration has presented the $m_{K^+K^-}$ distributions for the signal events splitted according to the sign of $\cos\theta_H$, where θ_H is the helicity angle. For the $B^\mp \rightarrow K^\mp(p_1)K^\pm(p_2)K^\mp(p_3)$ decay θ_H is defined in the center-of-mass frame of the $K^\pm(p_2)K^\mp(p_3)$ mesons as the angle between the two same-sign charge kaons. The variables s_{12} and s_{23} are related to $\cos\theta_H$ in the following way:

$$s_{12} = \frac{1}{2}(M_B^2 - s_{23} + 3m_K^2) + 2|\vec{p}_1||\vec{p}_2|\cos\theta_H, \quad (34)$$

where the moduli of the momenta $|\vec{p}_1^\rightarrow|$ and $|\vec{p}_2^\rightarrow|$ are given in Eq. (29). Then from Eqs. (28) one can see that the lower limit of s_{12} corresponds to $\cos \theta_H = -1$ while s_{12max} corresponds to $\cos \theta_H = +1$.³

Using the above definitions of s_{12} limits we are able to split the m_{23} distribution from Eq. (27) into two parts corresponding to $\cos \theta_H < 0$

$$\frac{dBr^\pm(\cos \theta_H < 0)}{dm_{23}} = 4 m_{23} \int_{DL}^{GL} ds_{12} \frac{dBr^\pm}{ds_{12} ds_{23}} \quad (35)$$

or to $\cos \theta_H > 0$

$$\frac{dBr^\pm(\cos \theta_H > 0)}{dm_{23}} = 4 m_{23} \int_{DG}^{s_{12max}} ds_{12} \frac{dBr^\pm}{ds_{12} ds_{23}}. \quad (36)$$

The lower limit DL of the first integral equals to s_{12min} for $2m_K < m_{23} < d$ and $DL = s_{23}$ for $d < m_{23} < m_0 \equiv \sqrt{M_B^2/3 + m_K^2} \approx 3.0877$ GeV. The upper limit is given by $GL = (M_B^2 - s_{23} + 3m_K^2)/2$. Finally the lower limit DG in Eq. (36) equals to GL for $2m_K < m_{23} < m_0$ or $DG = s_{23}$ if $m_0 < m_{23} < g$.

4 Data selection, the fitting method and additional parameters in the model

Three data sets of the $B^\pm \rightarrow K^\pm K^+ K^-$ decays measured by the *BABAR* (Ref. [16]) and by the LHCb collaborations (Refs. [19], [20] and [21]) are simultaneously analysed. The effective $K\bar{K}$ mass distributions $m_{K+K^- low}$, $m_{K+K^- high}$ and m_{K+K^+} presented by *BABAR* on Figs. 7 and 8 of [16] and the LHCb projections from Fig. 6 of [19], from Fig. 2 of [20] and from Fig. 7(a) of [21] are chosen for a comparison with the theoretical calculations based on the model described in Secs. 2 and 3. The model parameters have also been constrained by the experimental branching fraction of the $B^+ \rightarrow K^+ K^- K^+$ decay: $Br_{exp} = (3.40 \pm 0.14) \times 10^{-5}$ [26]. Another constraint has been related to the experimental value of the branching fraction for the decay of B^+ into $K^+ \phi$ multiplied by the secondary branching fraction for the decay of ϕ into the $K^+ K^-$ pair (Ref. [26]). The resulting value for the $B^+ \rightarrow K^+ K^- K^+$ decay in the range of the $m_{K+K^- low}$ mass where the P -wave $\phi(1020)$ resonance dominates has been taken as $Br_{exp}^P = (4.33 \pm 0.34) \times 10^{-6}$. This value has been compared to the integral of the theoretical branching fraction distribution $\frac{dBr^+}{dm_{23}}$ over the mass range between the $K^+ K^-$ threshold and 1.05 GeV. However, in this case we have only included the P -wave amplitudes A_3^+ and A_4^+ in the amplitude $A_{sym}^+(s_{12}, s_{23})$ (see Eq. 26).

³We have noticed a disagreement between the definition of the helicity angle and the captions of Figs. 4, 5 and 6 given in Ref. [19], namely the figures corresponding to the regions of $\cos \theta_H > 0$ and $\cos \theta_H < 0$ have been interchanged. Therefore (for example) the third line of Fig. 6 caption should read: "The plots are restricted to events with (a),(c) $\cos \theta > 0$ and (b), (d) $\cos \theta < 0$." The necessity of this change has been confirmed by Irina Nasteva (Ref. [31]).

In order to make a comparison of the experimental Dalitz plot projections with our model we have eliminated a few experimental data points corresponding to the $K\bar{K}$ masses in bins with the central values below the nominal K^+K^- threshold mass or the masses which can be attributed to the decays of the D^0 , J/Ψ , χ_{c0} and $\Psi(4360)$ mesons to K^+K^- . Here we note that the above decays are not included in the present model.

The theoretical branching fraction distributions defined in Sec. 3 have been multiplied by the normalization factors defined as the ratios of the B^\pm signal yields to the total branching fraction Br_{exp} . For the *BABAR* data [16] the number of signal events is equal to 5269. According to the LHCb data from Figs. 2(a) and 2(b) of Ref. [20] a sum of the B^+ and B^- signal events is 103211 and this number is used to calculate the corresponding normalization factor. The normalization factor of the LHCb data from Fig. 7(a) in [21] is calculated as a ratio of the sum of the B^+ and B^- signal events to the theoretical branching fraction integrated over the $m^2(K^+K^-)_{high}$ distribution while the $m^2(K^+K^-)_{low}$ region is limited by the 1.1 GeV² and 2.25 GeV² values. One bin corresponding to J/Ψ and three bins around the χ_{c0} position have been subtracted from the data set.

Altogether 318 *BABAR* data bins, 256 LHCb bins from [19] and [20], and 142 bins from [21] have been taken into account, so the total number of the data bins was equal to 716. The χ^2 distribution method has been used to fit all these data and in addition the two total branching fractions Br_{exp} and Br_{exp}^P . In order to get a better normalization of the model amplitudes to the full data set the χ^2 values for these two last data have been multiplied by a factor of ten .

After performing some preliminary fits to data we realized that the initial set of 17 model parameters is not sufficient to describe well the Dalitz plot projection distributions, especially for the high effective $K\bar{K}$ masses above 1.8 GeV. This is a region where our knowledge of the kaon-kaon interactions is very limited, in particular in the S -wave. Thus we have modified the functional dependence of two S -wave amplitudes A_1^- and A_2^- on the s_{23} variable. The kaon strange scalar form factor $\Gamma_2^{s*}(s_{23})$ in Eq. (3) has been multiplied by the following polynomial

$$P_s(x) = \left(1 + \sum_{i=1}^6 c_i x^i\right) f_1, \quad x = m_{23} - 2m_K, \quad (37)$$

where c_i are real coefficients, f_1 is complex and we remind that $m_{23} = \sqrt{s_{23}}$. This polynomial is normalized to 1 at the K^+K^- threshold. Similarly the kaon non-strange scalar form factor $\Gamma_2^{n*}(s_{23})$ in Eq. (4) has been multiplied by the polynomial $P_n(x)$:

$$P_n(x) = 1 + \sum_{i=1}^6 d_i x^i, \quad (38)$$

where d_i are also real coefficients. Finally we multiply the transition function $G_1(s_{23})$

Table 1: Parameters of our model amplitudes. Phases are given in radians.

Amplitude parts	Parameter	modulus	phase
A_1	f_1	0.60371	-0.0504
A_2	χ	1.4729 GeV ⁻¹	-1.4484
A_2	r_2	11.166 GeV ^{3/2}	-2.4061
A_3, A_4	b_1	4.0331	2.8885
A_3, A_4	b_2	0.19908	-2.0
A_3, A_4	b_3	0.14769	0.5230
A_3	b_ϕ	1.1524	3.1416
A_5	F_5	0.15961	0.0793
A_6	F_6	1.0192	2.9281

by the polynomial $P_G(x)$

$$P_G(x) = 1 + \sum_{i=1}^6 g_i x^i, \quad (39)$$

where g_i are new real parameters.

The same polynomials $P_s(x)$, $P_n(x)$ and $P_G(x)$ have been introduced in the B^+ decay amplitude $A^+(s_{12}, s_{23})$. Addition of these polynomials in the S -wave amplitudes has led us to a substantial improvement of the theoretical distributions on the Dalitz plot. The total number of free parameters equals to 35.

5 Results

The parameters obtained in the data fit are given in Table 1 and the coefficients of the polynomials defined in Eqs. (37-39) can be found in Table 2. The theoretical value of the total averaged branching fraction for the $B^\pm \rightarrow K^\pm K^- K^+$ decays equal to $Br^{th} = 3.33 \times 10^{-5}$ is very close to the experimental branching fraction $Br^{exp} = (3.40 \pm 0.14) \times 10^{-5}$. Also the total branching fraction integrated over the $K^+ K^-$ effective mass up to 1.05 GeV, where the $\phi(1020)$ resonance dominates, has been calculated. Its value 4.45×10^{-6} lies well within one standard deviation from the experimental value $(4.33 \pm 0.34) \times 10^{-6}$.

The Dalitz plot projections obtained from our model and compared with the corresponding *BABAR* data [16] are shown in Figs. 2-4. The theoretical distributions compared with the LHCb data sets [19], [20] and [21] can be found in Figs. 5-8.

Table 2: Coefficients of polynomials in our model amplitudes (Eqs. 37 - 39). Dimensions of the coefficients are GeV^{-i} , where the index $i = 1, \dots, 6$.

Index	polynomial $P_s(x)$	polynomial $P_n(x)$	polynomial $P_G(x)$
i	c_i	d_i	g_i
1	-0.57635	-7.2486	2.1473
2	-2.3976	-4.6746	-0.10438
3	3.7440	32.407	1.4636
4	-1.3362	-22.732	4.6728
5	.052993	4.4602	-3.6713
6	.017296	-0.16001	0.56857

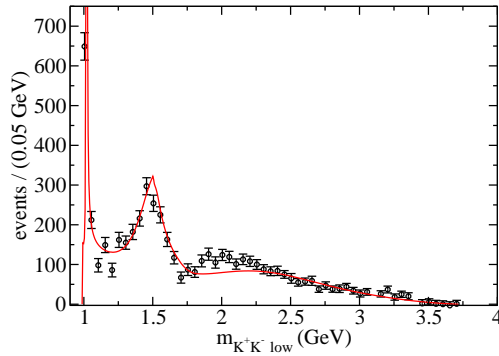


Figure 2: Distribution of $m_{K^+K^- \text{ low}}$. The *BABAR* Collaboration data points are taken from Fig. 7 of Ref. [16]. The line is calculated from our model by adding the B^- and B^+ distributions given by Eq. (27).

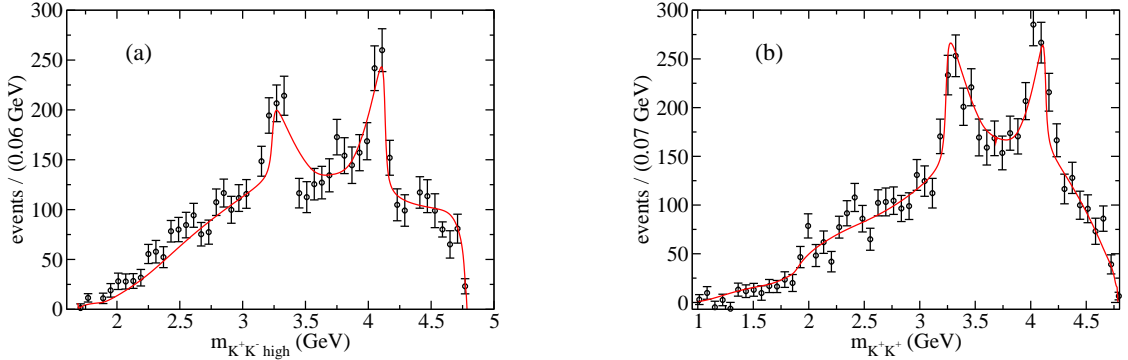


Figure 3: Distributions of $m_{K^+K^- \text{ high}}$ (a) and $m_{K^+K^+}$ (b). The *BABAR* Collaboration data points are taken from Fig. 7 of Ref. [16]. The lines are calculated from our model by adding the B^- and B^+ distributions given by Eq. (30) for the case (a) and by Eq. (33) for the case (b).

The theoretical total branching fractions $Br^{th}(B^+)$ and $Br^{th}(B^-)$ are calculated by the Dalitz plot integration of the differential branching fractions for the $B^+ \rightarrow K^+K^+K^-$ and the $B^- \rightarrow K^-K^+K^-$ decays, respectively. We have obtained $Br^{th}(B^+) = 3.48 \times 10^{-5}$ and $Br^{th}(B^-) = 3.19 \times 10^{-5}$. Then the direct CP asymmetry defined as

$$A_{CP} = \frac{Br^{th}(B^-) - Br^{th}(B^+)}{Br^{th}(B^-) + Br^{th}(B^+)} \quad (40)$$

takes the value $A_{CP} = -4.5\%$. This number can be compared with the experimental value of the *BABAR* Collaboration $(-1.7^{+1.9}_{-1.4} \pm 1.4)\%$ [16] and the LHCb results $(-3.6 \pm 0.4 \pm 0.2 \pm 0.7)\%$ from [19] and $(-3.7 \pm 0.2 \pm 0.2 \pm 0.3)\%$ from [21].

It is interesting to determine contributions to the total branching fraction of the different decay amplitudes grouped according to the relative spin of the K^+K^- pair. Thus in Table 3 we show the averages of the integrated branching fractions for the B^+ and B^- decays calculated separately for the S -, P - and D - waves. Also the ratios to the value of the branching fraction Br^{th} are given. We see that the S -wave amplitudes dominate, the P -wave amplitudes are also important, but the D -wave ones are small. From the numbers shown in this table we can deduce that the interference terms between the S -, P - and D - parts amount to a negative value of -29.2% .

We have also studied the interference effects appearing in the contributions to the branching fraction coming from the S -wave amplitudes (see Eqs. (3) and (4)). Let us denote by Br_S the average of the S -wave branching fractions for the B^+ and B^- decays. Then one can separately calculate the contributions to Br_S of the isospin zero and isospin one S -wave amplitudes. The isospin zero amplitude is the sum of the A_1 amplitude given by Eq. (3) and the first term of the amplitude A_2

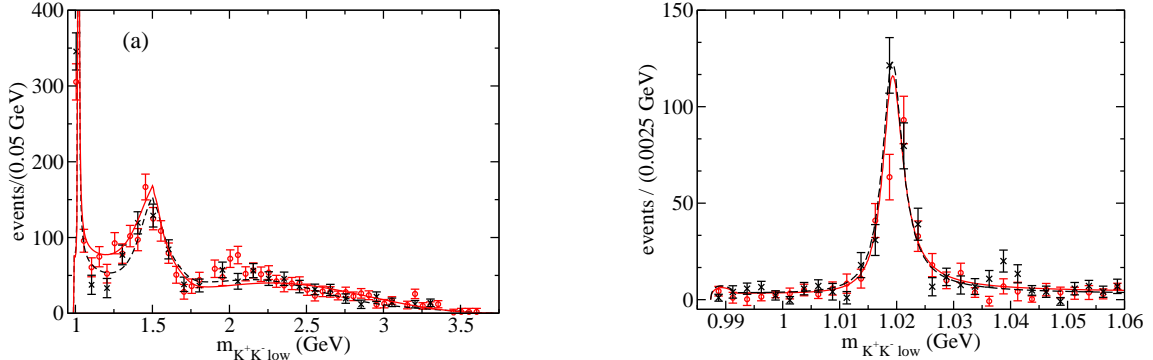


Figure 4: Distribution of $m_{K^+K^- \text{ low}}$ in the full mass region (a) and in the mass range restricted to 1.06 GeV (b). The *BABAR* Collaboration data points for the $B^\pm \rightarrow K^\pm K^+ K^-$ decays are taken from Fig. 8 of Ref. [16]. The red points correspond to the B^+ decays while the black ones to the B^- events. The red continuous lines represent the results of our model for the B^+ decays and the black dashed lines correspond to the B^- decays.

in Eq. (4) which is proportional to the non-strange kaon form-factor $\Gamma_2^{m*}(s_{23})$. The isospin one amplitude is proportional to the $G_1(s_{23})$ function seen in Eq. (4). In Table 4 we present the two isospin branching fractions as well as the sizable value of the interference term between these isospin amplitudes. In the isospin zero case the amplitude A_1 gives 1.44×10^{-5} contribution while the isospin one term adds 0.58×10^{-5} to the corresponding branching fraction. The interference term between these isospin parts of the amplitude is positive and large as it constitutes about 30% of the total rate in comparison with about 50% and 20% relative ratios of the isospin zero and one, respectively.

In the last column of Table 3 one finds the CP asymmetries. The largest asymmetry is obtained for the P -wave amplitudes. The CP asymmetries for the S - and D - states integrated over the full Dalitz plot are smaller. However, this does not mean that there do not exist regions in the Dalitz plot where the CP asymmetry is large. Indeed, in 2011 in Ref. [13] before a publication of the *BABAR* [16] and the LHCb data [19] we have predicted a large CP asymmetry. It is particularly well visible in Figs. 5(a) and 6(a) for the $m_{K^+K^- \text{ low}}$ mass range below 1.4 GeV. This negative asymmetry is larger for the range of the helicity angles in which $\cos \theta_H$ is negative. This is shown in more detail in Table 5 where the B^\pm branching fractions and CP asymmetries in the regions of the negative and positive values of $\cos \theta_H$ as well as in the full range of helicity angles are presented. A closer insight in the origin of these large CP asymmetries indicates an essential role of the $\rho(770)$ and the $\rho(1450)$ resonance contributions which are present in the P -wave amplitudes A_3 and A_4 (Eqs. (5) and (6)). Here the interference effects between the S - and P -waves

Table 3: Averages of the branching fractions for the B^+ and B^- decays corresponding to separate S -, P - and D -wave K^+K^- amplitudes. In the 4th column ratios of these averages to the total averaged branching fraction $Br^{th} = 3.33 \times 10^{-5}$ are given. The 5th column contains the CP asymmetries.

Amplitudes	wave	$\frac{1}{2}[Br(B^+)+Br(B^-)]$	ratio to Br^{th} in %	A_{CP} in %
A_1+A_2	S	2.89×10^{-5}	86.6	-2.2
A_3+A_4	P	1.36×10^{-5}	40.8	-9.7
A_5+A_6	D	0.59×10^{-6}	1.8	-0.9
	sum	4.31×10^{-5}	129.2	-4.5

Table 4: Contributions of the isospin zero and one S -wave amplitudes and its interference to the average Br_S of the S -wave branching fractions for the B^+ and B^- decays.

	branching fraction	ratio to Br_S in %
isospin 0	1.44×10^{-5}	49.8
isospin 1	0.58×10^{-5}	19.9
interference term	0.87×10^{-5}	30.3
Br_S	2.89×10^{-5}	100.0

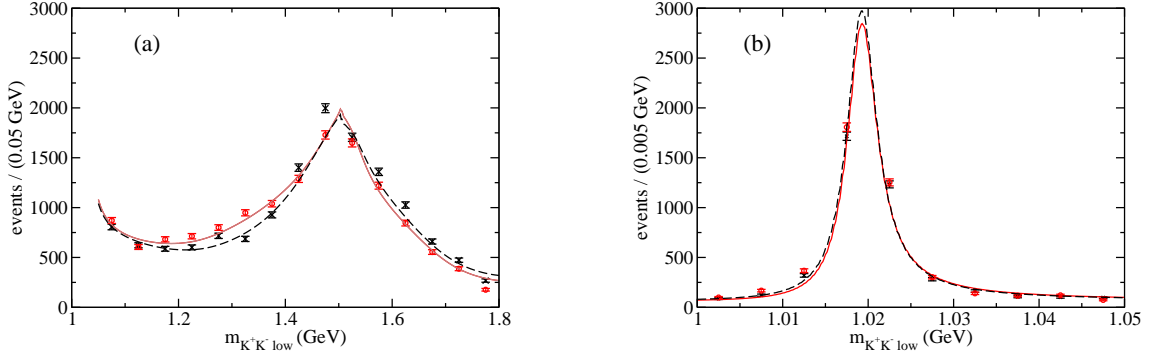


Figure 5: Distributions of the $m_{K^+K^- low}$ variable in the mass region up to 1.8 GeV (a) and in the mass range dominated by the $\phi(1020)$ resonance (b). The LHCb Collaboration data for the $B^\pm \rightarrow K^\pm K^+ K^-$ decays are taken from Fig. 6(a) of Ref. [19]. The events are chosen from the range $\cos \theta_H > 0$, where θ_H is the helicity angle. The red points correspond to the B^+ decays while the black ones to the B^- events. The continuous red lines are calculated from our model for the B^+ decays while the black dashed ones for the B^- decays.

are important.

In Fig. 5(a) one can see a change of sign of the CP asymmetry starting from the $m_{K^+K^- low}$ mass exceeding about 1.4 GeV. This feature of the LHCb data is well reproduced by our model. The case of $\cos \theta_H > 0$ shown in Fig. 6(a) for $m_{K^+K^- low} > 1.5$ GeV is less clear. First of all the data for both the B^+ and B^- decays have somewhat irregular behaviour at $m_{K^+K^- low}$ in vicinity of 1.5 GeV. One can also notice that the three B^+ decay data points at $m_{K^+K^- low}$ around 1.6 GeV lie above the corresponding theoretical curve. However, an inspection in Fig. 2 of Ref. [19] can lead to a guess that this behaviour is related to a kind of interference effects in the Dalitz plot distributions due to a presence of the horizontal band of events related to the χ_{c0} decays into the K^+K^- pairs. These χ_{c0} decays cannot influence the distributions of events with $\cos \theta_H > 0$ and we see that in Fig. 5 the mass distributions are more smooth than those seen in Fig. 6. In our model we do not describe the decays $B^\pm \rightarrow K^\pm \chi_{c0}$, so some deviation from the data in that rather narrow mass range can be expected but only for $\cos \theta_H < 0$.

In Fig. 7 two Dalitz plot projections of the $m(K^+K^-)_{high}$ and $m(K^+K^-)_{low}$ variables are given. The theoretical curves describe well the experimental data of the LHCb Collaboration presented in [20]. Two maxima seen in Fig. 7(a) correspond mainly to the $B^\pm \rightarrow \phi(1020)K^\pm$ decay events. The same events are grouped in a very narrow peak near 1 GeV in Fig. 7(b). The other maximum seen at about 1.5 GeV can be explained as a combined effect of the existence of the three maxima present in the strange $\Gamma_2^{s*}(s_{23})$, non-strange $\Gamma_2^{n*}(s_{23})$ scalar kaon form factors and

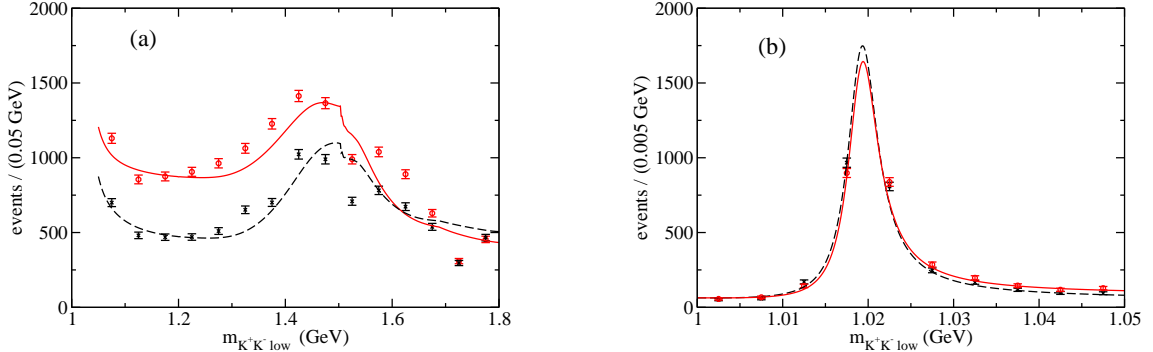


Figure 6: Distributions of the $m_{K^+K^- low}$ variable in the mass region up to 1.8 GeV (a) and in the mass range dominated by the $\phi(1020)$ resonance (b). The LHCb Collaboration data for the $B^\pm \rightarrow K^\pm K^+ K^-$ decays are taken from Fig. 6(b) of Ref. [19]. The events are chosen from the range $\cos \theta_H < 0$, where θ_H is the helicity angle. The red points correspond to the B^+ decays while the black ones to the B^- events. The continuous red lines are calculated from our model for the B^+ decays while the black dashed ones for the B^- decays.

in the transition function $G_1(s_{23})$. These functions are present in the amplitudes A_1 and A_2 (Eqs. (3) and (4)). The three scalar resonances $f_0(1370)$, $f_0(1500)$ and $a_0(1450)$ play a role in an appearance of the above mentioned maximum at 1.5 GeV. One may also ask as in Ref. [6] what is a role of the resonance $\rho(1450)$. We have performed a special calculation of the $\rho(1450)$ contribution to the height of the $m(K^+K^-)_{low}$ maximum in Fig. 7(b). The relative values of this contribution with respect to the experimental numbers of events vary between 3% and 4% for the B^- and B^+ decays, respectively. So our conclusion is that the $\rho(1450)$ resonance alone is not responsible for the maximum seen at about 1.5 GeV.

In Fig. 8 we show a comparison of the $m^2(K^+K^-)_{high}$ projections with the re-

Table 5: Branching fractions for the B^+ and B^- decays integrated over the $m_{K^+K^- low}$ mass range between 1.05 GeV and 1.4 GeV and the corresponding CP asymmetries in the three ranges of the helicity angle θ_H .

range of $\cos \theta_H$	$Br(B^-)$	$Br(B^+)$	A_{CP} in %
$\cos \theta_H < 0$	2.50×10^{-6}	4.35×10^{-6}	-26.9
$\cos \theta_H > 0$	3.29×10^{-6}	3.65×10^{-6}	-5.2
full	5.79×10^{-6}	8.0×10^{-6}	-16.0

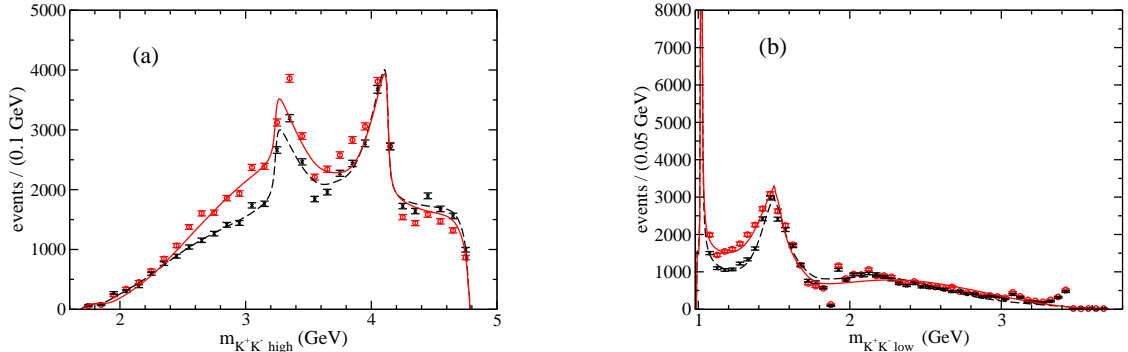


Figure 7: Distributions of the $m_{K^+K^-}^{high}$ variable (a) and the $m_{K^+K^-}^{low}$ variable (b). The LHCb Collaboration data for the $B^\pm \rightarrow K^\pm K^+ K^-$ decays are taken from Fig. 2 of Ref. [20]. The red points correspond to the B^+ decays while the black ones to the B^- events. The continuous red lines are calculated from our model for the B^+ decays while the black dashed ones for the B^- decays.

cent LHCb data (Fig. 7(a) of [21]). These projections correspond to the so-called rescattering region defined as a rather narrow band on the Dalitz plot obtained by limiting the $m^2(K^+K^-)_{low}$ values between 1.1 GeV² and 2.25 GeV². One observes a strong negative CP asymmetry for the $m^2(K^+K^-)_{high}$ values lower than about 17 GeV². The mass projections corresponding to the B^+ and B^- decays are rather well described by the model except of a few points at $m^2(K^+K^-)_{high}$ values near 9.6 and 11.7 GeV² corresponding to the J/Ψ and χ_{c0} decays. Let us notice that the negative CP asymmetry effect seen in this figure is also present in Fig. 6(a) for the $m(K^+K^-)_{low}$ values smaller than 1.5 GeV.

6 Summary and final comments

We have analysed decays of the B^\pm mesons into three charged kaons $K^\pm K^+ K^-$. The decay amplitudes have been constructed in the framework of the QCD factorization model and then used to describe the kaon distributions in the whole Dalitz plot. The model parameters have been simultaneously fitted to the data of the *BABAR* and LHCb collaborations and a good agreement has been obtained in a description of the $K\bar{K}$ effective mass distributions in their full kinematical ranges. The strong interactions between the K^+ and K^- mesons have been taken into account. These interactions can have a resonant character for lower effective masses starting from the $K\bar{K}$ threshold. Many resonances which can decay to K^+K^- pairs in the S -, P - and D -waves give contributions to the decay amplitudes.

At higher effective masses above about 2 GeV the KK interactions may have

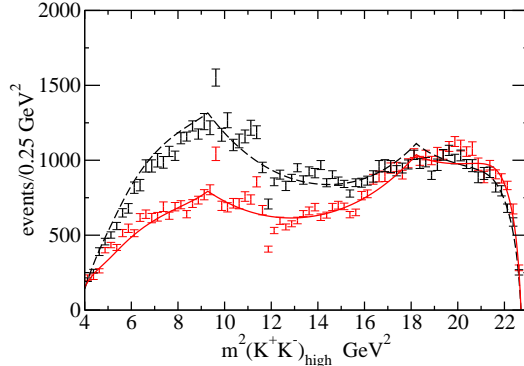


Figure 8: Distributions of the $m_{K^+K^-}^{high}$ variable. The LHCb Collaboration data for the $B^\pm \rightarrow K^\pm K^+ K^-$ decays are taken from Fig. 7(a) of Ref. [21]. The red points correspond to the B^+ decays while the black ones to the B^- events. The results of our model are represented by the red line for the B^+ decays and by the black dashed line for the B^- decays.

non-resonant features and in our model we have parameterized them in terms of the polynomials included in the S -wave amplitudes. The Dalitz-plot distributions are dominated by these S -wave contributions. The P -wave amplitudes are especially important at low K^+K^- masses with the $\phi(1020)$, $\rho(770)$ and $\rho(1450)$ resonances interfering strongly with the S -wave amplitudes. The interference effects depend on the B meson charges leading to the CP asymmetry which varies significantly over the Dalitz-plot. Generally the CP asymmetry is negative in the Dalitz-plot range limited from one side by the effective mass $m_{K^+K^-}^{low}$ smaller than about 1.6 GeV and by the $m_{K^+K^-}^{high}$ smaller than about 3.7 GeV from the second side. In other parts of the Dalitz-plot the CP asymmetry is mostly positive and this leads to rather small negative integrated asymmetry equal to -4.5%.

An important comment should be made here. The particle distributions on the Dalitz-plot, the $m_{K^+K^-}^{low}$ and $m_{K^+K^-}^{high}$ projections and in particular the CP asymmetry distributions cannot be analysed and understood without taking into account the symmetrization properties of the decay amplitudes as written in Eq. (1). This symmetrization leads to a rich structure of the above mentioned functions of two variables s_{23} and s_{12} . In particular, one cannot interpret the interference effects of the S - and P -wave decay amplitudes using an assumption that the S -wave amplitude depends only on the s_{23} variable and the P -wave amplitude is a function of s_{23} multiplied by the cosine of the helicity angle θ_H . The symmetrization effects, numerically large in the most parts of the Dalitz-plot, make this assumption not valid.

ACKNOWLEDGEMENTS

We would like to thank Irina Nasteva for a correspondence concerning the LHCb data. We are also grateful to Bachir Moussallam for a calculation of the kaon form factor values and for many useful discussions.

References

- [1] H.Y. Cheng and C. K. Chua, Branching fractions and direct CP violation in charmless three-body decays of B Mesons, Phys. Rev. D **88**, 114014 (2013).
- [2] H.Y. Cheng, C.K. Chua, and Z. Q. Zhang, Direct CP violation in charmless three-body decays of B Mesons, Phys. Rev. D **94**, 094015 (2016).
- [3] Z.T. Zou, Y. Li, Q.X. Li, and X. Liu, Resonant contributions to three-body $B \rightarrow KKK$ decays in perturbative QCD approach, Eur. Phys. J. C **80**, 394 (2020).
- [4] Y. Y. Fan and W. F. Wang, Resonance contributions $\phi(1020, 1680) \rightarrow KK^-$ for the three-body decays $B \rightarrow K\bar{K}h$, Eur. Phys. J. C **80**, 815 (2020).
- [5] W. F. Wang, Contributions for the kaon pair from $\rho(770)$, $\omega(782)$ and their excited states in $B \rightarrow K\bar{K}h$ decays, Phys. Rev. D **103**, 056021 (2021).
- [6] Z.T. Zou, Y. Li, and H.n. Li, Is $f_X(1500)$ observed in the $B \rightarrow \pi(K)KK$ decays $\rho^0(1450)$?, Phys. Rev. D **103**, 013005 (2021).
- [7] A. Furman, R. Kamiński, L. Leśniak, and B. Loiseau, Long-distance effects and final state interactions in $B \rightarrow \pi\pi K$ and $B \rightarrow K\bar{K}K$ decays, Phys. Lett. B **622**, 207 (2005).
- [8] J.H. Alvarenga Nogueira, I. Bediaga, A.B.R. Cavalcante, T. Frederico, and O. Lourenço, CP violation: Dalitz interference, CPT and final state interactions, Phys. Rev. D **92**, 054010 (2015).
- [9] I. Bediaga, T. Frederico, P. C. Magalhães, and D. T. Machado, Global CP asymmetries in charmless three-body B decays with final state interactions, Phys. Lett. B **824**, 136824 (2022).
- [10] R. Álvarez Garrote, J. Cuervo, P.C. Magalhães, and J.R. Peláez, Dispersive $\pi\pi \rightarrow K\bar{K}$ Amplitude and Giant CP Violation in B to Three Light-Meson Decays at LHCb, Phys. Rev. Lett. **130**, 201901 (2023).
- [11] I. Bediaga, T. Frederico, and P.C. Magalhães, Charm Penguin in $B^\pm \rightarrow K^\pm K^+ K^-$: partonic and hadronic loops, Phys. Lett. B **780**, 357 (2018).

- [12] T. Mannel, K. Olschewsky, and K.K. Vos, CP violation in three-body B decays: a model ansatz, *J. High Energy Phys.* 06, 073 (2020).
- [13] A. Furman, R. Kamiński, L. Leśniak, and P. Żenczykowski, Final state interactions in $B^\pm \rightarrow K^+K^-K^\pm$ decays, *Phys. Lett. B* **699**, 102 (2011).
- [14] L. Leśniak, and P. Żenczykowski, Dalitz-plot dependence of CP asymmetry in $B^\pm \rightarrow K^+K^-K^\pm$ decays, *Phys. Lett. B* **737**, 201 (2014).
- [15] A. Garmash *et al.* (Belle Collaboration), Dalitz analysis of the three-body charmless decays $B^+ \rightarrow K^+\pi^+\pi^-$ and $B^+ \rightarrow K^+K^+K^-$, *Phys. Rev. D* **71**, 092003 (2005).
- [16] J. P. Lees *et al.* (BABAR Collaboration), Study of CP violation in Dalitz-plot analyses of $B^0 \rightarrow K^+K^-K_S^0$, $B^+ \rightarrow K^+K^-K^+$, and $B^+ \rightarrow K_S^0K_S^0K^+$, *Phys. Rev. D* **85**, 112010 (2012).
- [17] R. Aaij *et al.* (LHCb Collaboration), Measurement of CP violation in the Phase Space of $B^\pm \rightarrow K^\pm\pi^+\pi^-$ and $B^\pm \rightarrow K^\pm K^+K^-$ Decays, *Phys. Rev. Lett.* **111**, 101801 (2013).
- [18] M. Benecke, M. Neubert, QCD factorization for $B \rightarrow PP$ and $B \rightarrow PV$ decays, *Nucl. Phys.* **B675**, 333 (2003).
- [19] R. Aaij *et al.* (LHCb Collaboration), Measurements of CP violation in the three-body phase space of charmless B^\pm decays, *Phys. Rev. D* **90**, 112004 (2014).
- [20] R. Aaij *et al.* (LHCb Collaboration), supplementary material, cds.cern.ch/record/1751517/files, LHCb-PAPER-2014-044 (2016).
- [21] R. Aaij *et al.* (LHCb Collaboration), Direct CP violation in charmless three-body decays of B^\pm mesons, *Phys. Rev. D* **108**, 012008 (2023).
- [22] P. Ball, and R. Zwicky, New results on $B \rightarrow \pi, K, \eta$ decay form factors from light-cone sum rules, *Phys. Rev. D* **71**, 014015 (2005).
- [23] R. Kamiński, L. Leśniak and B. Loiseau, Three channel model of meson-meson scattering and scalar meson spectroscopy, *Phys. Lett. B* **413**, 130 (1997).
- [24] R. Kamiński, L. Leśniak and B. Loiseau, Scalar mesons and multichannel amplitudes, *Eur. Phys. J. C* **9**, 141 (1999).
- [25] J.-P. Dedonder, R. Kamiński, L. Leśniak, and B. Loiseau, Dalitz plot studies of $D^0 \rightarrow K_S^0K^+K^-$ decays in a factorization approach, *Phys. Rev. D* **103**, 114028 (2021).

- [26] R.L. Workman *et al.*, Particle Data Group, Prog. Theor. Exp. Phys. 2022, 083C01 (2022).
- [27] B. Moussallam, private communication.
- [28] B. El-Bennich, O. Leitner, J.-P. Dedonder, and B. Loiseau, Scalar meson $f_0(980)$ in heavy-meson decays, Phys. Rev. D **79**, 076004 (2009).
- [29] C. Bruch, A. Khodjamirian, and J.H. Kühn, Modeling the pion and kaon form factors in the timelike region, Eur. Phys. J. C **39**, 41 (2005).
- [30] C. S. Kim, J.-P. Lee, and S. Oh, Nonleptonic two-body charmless B decays involving a tensor meson in the ISGW2 model, Phys. Rev. D **67**, 014002 (2003).
- [31] Irina Nasteva, private communication.